Reason - A Technical Journal
ISSN 2277–1654
Vol - XII • 2013

OPTIMIZATION OF PARAMETERS IN ELECTRICAL DISCHARGE MACHINING OF RENE80 NICKEL BASE SUPER ALLOY USING TAGUCHI-GREY RELATIONAL ANALYSIS

U. Shrinivas Balraj[1] and A. Gopalakrishna[2]

[1]Department of Mechanical Engineering, Kakatiya Institute of Technology and Science, Warangal, A.P., India. Email: u.shrinivas@gmail.com
[2]Department of Mechanical Engineering, JNTU College of Engineering, Kakinada, A.P., India. Email: dr.a.gopalakrishna@gmail.com

Paper received on: November 14, 2013, accepted after revision on: February 26, 2014.

Abstract: The paper deals with the electrical discharge machining of RENE80 nickel super alloy to investigate the effects of dominant process parameters like peak current, pulse on time and pulse off time on the output responses like radial overcut, tool wear rate and metal removal rate. The experiments are planned based on Taguchi method and optimal levels of process parameters are found out using signal to noise ratio. Significant parameters are identified using analysis of variance. It revealed that the responses are mainly affected by peak current and pulse on time. In addition, multi-objective optimization of all responses is done using Taguchi-grey relational analysis and found that peak current is dominant parameter followed by pulse on time and pulse off time respectively. Finally, surface topography analysis is done using SEM, EDAX and XRD and it indicates that there is no transfer of electrode material to the work piece and alterations in phases of the alloy.

Keywords: Electrical discharge machining, Taguchi-grey relational analysis, radial overcut, tool wear rate, metal removal rate.

1. INTRODUCTION

RENE80 nickel super alloy has high hardness (HRC 45), high strength and creep properties. It is difficult to machine due to low thermal conductivity and high affinity to react with the tool materials at high temperature generated during machining [1] and such alloy requires non-traditional machining processes such as electrical discharge machining (EDM). EDM is extensively used for machining complicated shapes and difficult to machine materials. Since EDM is an indispensable process in machining super alloys, it has been the centre of interest of several researchers to improve its performance in terms of dimensional/ geometrical accuracy, low electrode wear and high productivity [2]. Pradhan et al. [3] studied metal removal rate, tool wear rate, overcut and taper for EDM of titanium super alloy using Taguchi method and reported that pulse on time is the most influencing factor on MRR, overcut and taper. George et al. [4] determined optimal parameters of pulse current, gap Voltage and pulse on time for MRR and electrode wear rate while machining carbon-carbon composites using Taguchi approach. Kumar et al. [5] used Taguchi's experimental design to find optimal levels of current, pulse on time and pulse off time to maximize MRR and minimize relative wear ratio and surface roughness (SR) of maraging steel. Kao and Hsu [6] carried out optimization of EDM parameters on titanium alloy with multiple quality characteristics and improved material removal rate by 12% and reduced surface roughness and electrode wear ratio by 19% and 15% respectively using Taguchi method combined with grey relational theory. Aliakbari

and Baseri [7] used Taguchi method effectively to optimize machining parameters in rotary machining for responses like MRR, SR, electrode wear ratio and diametral overcut in EDM and reported that diametral overcut increases in rotary EDM. Singh et al. [8] investigated the effect of different electrode materials on the performance of EDM of EN-31 steel in relation to diametral overcut, electrode wear and surface roughness and concluded that copper is the better electrode material in terms of these responses. It is found from literature that limited work is reported on EDM of RENE80 nickel super alloy. Hence this study is carried out to find the effect of parameters dominant parameters like peak current, pulse on time and pulse off time on responses such as radial overcut (ROC), tool wear rate (TWR) and metal removal rate (MRR). In addition, multi-objective optimization is done using Taguchi-grey relational analysis (TGRA).

2. EXPERIMENTAL PROCEDURE

The chemical composition of work piece material RENE80 alloy in wt% is: Al 5-6; Cr 9.5-12; Ti 2.5-3.2; C 0.13-0.2; Mo 3.5-4.8; W 4.5-5.5; Co 4-4.5; B 0.02 max; Se 0.015 max; Si <0.4; Mn < 0.4; Fe 0.5 max; Ni balance. Pure electrolytic copper (99.97%) of diameter 14.3mm and density of 8.93g/cm^3 is used as electrode. The work pieces of the size 70 mm X 35 mm X 4 are used for experimentation. All experiments are conducted on die sink EDM (Make: ASKAR, model V3525, India) at experimental conditions given Table 1. The specifications of the dielectric fluid are given in Table 2. The parameters levels are shown in Table 3. An orthogonal array $L_9(3^4)$ is selected based on the number of degrees of freedom of parameters and pilot experiments and shown in Table 4. The Experiments are repeated three times at each parametric combination to reduce the noise error.

Table 1 Experimental conditions in EDM

Work piece	70mm X 35mm X 4mm plate
Electrode	Electrolytic copper tool (diameter=14.3mm)
Dielectric	Rustlick commercial EDM oil (grade 30)
Dielectric flushing	Side flushing with pressure
Dielectric pressure	0.5 MPa (constant under whole conditions)
Polarity	Positive (work piece '+ve' and tool '–ve')
Work time	3 minutes
Gap	≈70µm (default value)
Gap Voltage	30V (constant)

Table 2 Physical and chemical properties of EDM-grade 30 oil

Property	State/value
Physical state	Liquid
Colour	Clear, Colourless
Odour	Mild
Viscosity	3.5 cSt
Boiling point	150^{0}C
Solubility in water	Insoluble
Specific gravity	0.80

Table 3 Process Parameter Levels

Input parameters	Peak Current	Pulse on time	Pulse off time
Symbol	A	B	C
Level1	6	10	10
Level2	15	20	20
Level3	24	50	50

Table 4 $L_9(3^4)$ - Orthogonal Array

No	A	B	C
1	1	1	1
2	1	2	2
3	1	3	3
4	2	1	2
5	2	2	3
6	2	3	1
7	3	1	3
8	3	2	1
9	3	3	2

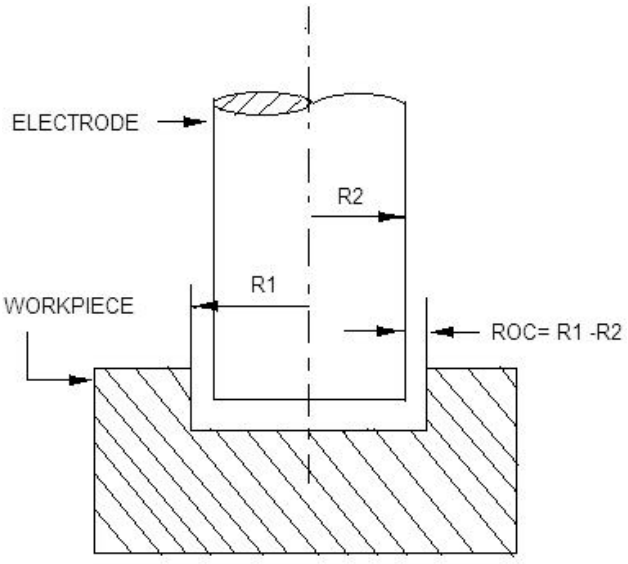

Fig. 1 Measurement of ROC

The weights of work pieces are measured with digital balance (Make: Shimadzu Philippines, Japan and accuracy-1mg). TWR and MRR are measured by taking the difference between the weights of tool and electrode before and after machining and dividing by machining time. Optical microscope (Make: Mitutoyo, accuracy -1µm) is used to measure the diameter of the machined hole in two perpendicular directions per each trial. ROC is measured as the difference between the average radius of machined hole and radius of the electrode before machining as shown in Fig. 1 [9],

$$ROC = (R1 - R2)\ mm \qquad (1)$$

where

R1 = average radius of the machined hole

R2 = radius of the electrode

2.1. Design of Experiments Based on Taguchi Method

Taguchi's method is very effective to deal with responses affected by many process parameters. In this, the experimental values of various responses are transformed into signal to noise (S/N) ratio. The response that is to be maximized is called 'Higher the better' and the response that is to be minimized is called 'Lower the better'. Taguchi uses the S/N ratio to measure deviation of the response from the mean value. S/N ratios for 'Higher the better' and 'Lower the better' characteristics are calculated using equations 2 and 3 respectively,

$$\eta = -10\log_{10}\left[\frac{1}{n}\sum_{i=2}^{n}\frac{1}{y_i^2}\right] \qquad (2)$$

$$\eta = -10\log_{10}\left[\frac{1}{n}\sum_{i=2}^{n}y_i^2\right] \qquad (3)$$

where, η denotes S/N ratio of experimental values, y_i represents the experimental value of the i^{th} experiment and n is total number of experiments.

3. RESULTS AND DISCUSSION

The experimental results and S/N ratios of ROC, TWR and MRR are shown in Table 5 and Table 6 respectively. The effect of parameters

Table 5 Experimental values and S/N ratios (dB) of ROC

No	Machined hole diameters						Average diameter	ROC	S/N ratio
	Trial 1		Trial 2		Trial 3				
1	14.411	14.419	14.429	14.427	14.431	14.421	14.423	0.062	24.222
2	14.512	14.539	14.532	14.516	14.571	14.498	14.528	0.114	18.862
3	14.582	14.597	14.575	14.614	14.585	14.548	14.584	0.183	14.731
4	14.897	14.901	14.909	14.926	14.91	14.918	14.910	0.305	10.312
5	14.992	15.015	14.998	14.996	15.012	14.999	15.002	0.351	9.094
6	15.007	15.057	15.067	15.022	15.029	15.039	15.037	0.368	8.673
7	15.024	15.031	15.015	15.026	15.026	15.029	15.025	0.363	8.793
8	15.001	14.966	14.962	14.984	14.95	15.015	14.980	0.340	9.375
9	15.232	15.221	15.243	15.204	15.271	15.206	15.230	0.465	6.656

Table 6 Experimental values and S/N ratios (dB) of TWR and MRR

No.	TWR (mg/min.)				MRR (mg/min)			
	Trial1	Trial2	Trial3	S/N ratio	Trial1	Trial2	Trial3	S/N ratio
1	5.33	6.83	7.5	-16.329	59.50	56.33	53.83	35.0492
2	4.5	3.57	5.11	-12.856	79.20	81.71	88.83	38.4073
3	-0.5	1.5	1.83	0.510	105.5	113.6	101.2	40.5687
4	36.83	40.1	38.33	-31.691	288.3	279.5	280.5	49.0286
5	26.83	39.5	31.66	-30.281	365.3	355.3	362.6	51.1482
6	13.5	11.5	9.33	-21.171	390.0	407.5	376.5	51.8509
7	61.57	66.11	58.16	-35.840	475.5	470.5	448.0	53.3428
8	79.6	73.57	71.33	-37.482	396.5	391.5	379.5	51.7915
9	40.6	38.33	49.11	-32.604	524.5	533.3	556.5	54.6173

on responses is studied based on S/N ratios.

3.1. Effect of Process Parameters on ROC

Fig. 2(a) depicts the effects of process parameters on the average values of ROC. It is observed that ROC increases with all the three parameters but their degrees are varying. With increase of peak current and pulse on time, the primary discharge energy increases which occurs on the face of the tool electrode and removes more amount of material quickly from front side. But as the tool electrode progresses further into the work piece, secondary discharge takes place on the sidewall of the tool electrode. This secondary discharge also removes the material and

promotes increase in ROC [3]. Whereas with the increase of pulse off time, more amount of time is available for proper flushing of debris and melted molten material and this reduces the thickness of resolidified material on the face as well as sidewalls of the work piece and this results in increase in ROC.

3.2. Effect of Process Parameters on TWR

As shown in Fig. 2(b), TWR increases with the increase of peak current and it decreases with the increase of pulse on-time and pulse off time respectively. As the pulse energy increases with the increase of peak current which results in more number of electrons liberated from the electrode surface and impinge on the work piece surface. Hence the tool face wears at faster rate and it is found that TWR is increasing with increase of peak current almost linearly. At low pulse on time, the pulse energy is low and TWR is less. But with increase of pulse on time, the plasma channel formed is full and this results in increase of more material removal in the form of debris which is suspended in the machining zone. This debris gets deposited on the tool surface and obstructs further wear of the tool. In fact, this is detrimental to the removal of the material. Also the pyrolytic carbon particles formed due to break down of dielectric is more at high pulse on time and gets deposited on the tool face [10]. Hence the TWR decreases with increase of pulse on time. TWR is almost same at all levels of pulse off time.

3.3. Effect of Process Parameters on MRR

It can be observed from Fig. 2(c) that MRR increases with the increase of peak current, pulse on-time and pulse off time. The single pulse energy increases with an increase in peak current and pulse on-time and material removed by a single pulse increases and therefore, MRR increases. Generally no material is removed from the work piece during the pulse off time as there is no current, but Fig. 2(c) shows opposite of what was observed generally. MRR increases with pulse off time though small and insignificant because the dielectric gets sufficient time to flush away debris formed during the machining effectively and the machining process stabilizes and this observation is analogous to the work reported in [11].

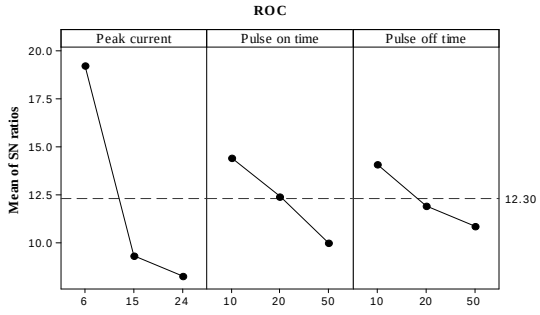

(a)

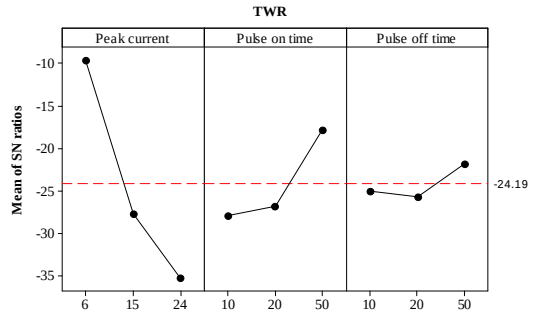

(b)

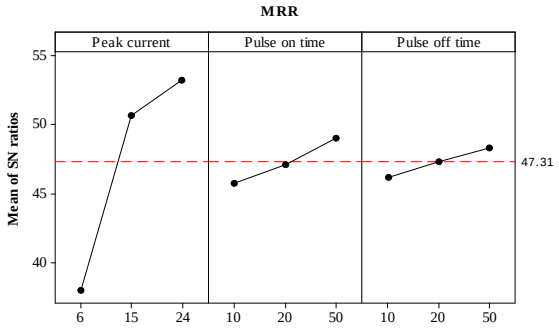

(c)

Fig.2 Main effects plots (a)ROC (b)TWR (c)MRR

4. MULTI-RESPONSE OPTIMIZATION USING TGRA

TGRA can be used to effectively solve complicated inter-relationships among multiple responses. It uses single weighted grey relational grade (WGRG) as performance index to determine optimal levels of parameters. In TGRA, the experimental results of ROC, TWR and MRR are first normalized in the range between 0 - 1 which is termed as grey relational generation. Various steps in TGRA [6] are as follows,

Step1: Find the normalized values of S/N ratios of responses. Linear normalization is usually required since the range and unit in one data sequence may be different from the other data sets. For smaller-the-better type, normalization of the response *i* is given by equation (4),

$$X_{ij}^{*} = \left(\frac{X_{ij} - \mathrm{Min}_j\left(X_{ij}\right)}{\mathrm{Max}_j\left(X_{ij}\right) - \mathrm{Min}_j\left(X_{ij}\right)} \right) \qquad (4)$$

For larger-the-better type, normalization of the response *i* is given by equation (5),

$$X_{ij}^{*} = \left(\frac{\mathrm{Max}_j\left(X_{ij}\right) - X_{ij}}{\mathrm{Max}_j\left(X_{ij}\right) - \mathrm{Min}_j\left(X_{ij}\right)} \right) \qquad (5)$$

where, X_{ij}^{*} is the normalized S/N ratio value after grey relational generation in the j^{th} experiment for j =1,2,...,q

Step 2: Find the maximum (R) of normalized values regardless of responses.

$$R = \mathrm{Max}\,(X_{ij}^{*}) \qquad (6)$$

Step 3: Find the absolute difference (Δ_{ij}) between each normalized value and R regardless of the responses,

$$\Delta_{ij} = | X_{ij}^{*} - R | \qquad (7)$$

Step 4: Find grey relational coefficient (ξ_{ij}) for each of normalized values using equation (8)

$$\xi_{ij} = \left(\frac{\mathrm{min}_i\, \mathrm{min}_j\left(\Delta_{ij}\right) + \xi \mathrm{Max}_i \mathrm{Max}_j\left(\Delta_{ij}\right)}{\Delta_{ij} + \xi \mathrm{Max}_i \mathrm{Max}_j\left(\Delta_{ij}\right)} \right) \qquad (8)$$

where, ζ is the distinguishing coefficient and lies in the range 0 to 1. Its widely accepted value is 0.5.

Step 5**:** Find the WGRG (γ_j) for each j^{th} experiment using equation (9),

$$\gamma_j = \frac{1}{m}\left(\sum_{i=1}^{m} \sum_{j=1}^{q} w_i\, \xi_{ij} \right) \qquad (9)$$

where w_i is the weight for i^{th} response and m is number of responses,

$$0 < \gamma_j \leq 1 \text{ and } \sum_{i=1}^{m} w_i = 1$$

Step 6: Find the optimal level of each parameter based on larger-the-better type response.

Step 7: Perform ANOVA using WGRGs of experiments and draw the inferences.

Step 8: Conduct confirmation experiments and verify the results.

Table 7 Normalized S/N ratios and WGRG values

No	Normalized S/N ratios			Grey relational coefficients			WGRG	Order
	ROC	TWR	MRR	ROC	TWR	MRR		
1	1	0.557	0	1	0.530	0.333	0.205	2
2	0.695	0.648	0.172	0.621	0.587	0.376	0.174	6
3	0.460	1	0.282	0.481	1	0.411	**0.208**	**1**
4	0.208	0.152	0.714	0.387	0.371	0.636	0.153	9
5	0.139	0.190	0.823	0.367	0.382	0.738	0.164	7
6	0.115	0.429	0.859	0.361	0.467	0.780	0.177	4
7	0.122	0.043	0.935	0.363	0.343	0.885	0.175	5
8	0.155	0	0.856	0.372	0.333	0.776	0.163	8
9	0	0.128	1	0.333	0.365	1	0.187	3

In this study, all the responses are equally weighted (0.33). Based on equations 8 and 9, the grey relational grade for each experiment is calculated. The normalized S/N ratios and WGRG values are shown in Table 7. Fig. 3 indicates the effect of each parameter on WGRGs. It shows that the predicted optimal parameter set is A1B3C3 based on TGRA. Table 8 shows the results of ANOVA of WGRGs. It is evident that the peak current is the significant control parameter affecting multiple responses followed by pulse on time and pulse off time respectively.

Table 8 ANOVA of WGRGs

Parameter	DF	Sum of squares	Mean sum of squares	F-test	Contribution (%)
A	2	0.001513	0.000756	7.49	54.58
B	2	0.000839	0.000419	4.15	30.25
C	2	0.000217	0.000109	1.07	7.87
error	2	0.000202	0.000101		7.30
Total	8	0.002770			100

Table 9 Results of confirmation experiments

Response	Optimal process parameters			
	Initial data A1B2C1	Prediction A1B3C3	Experiment A1B3C3	Improvement %
ROC	0.159	-	0.184	-15.72
TWR	3.61	-	0.9433	73.86
MRR	78.53	-	106.76	35.94
WGRG	0.1833	0.2130	-	16.20

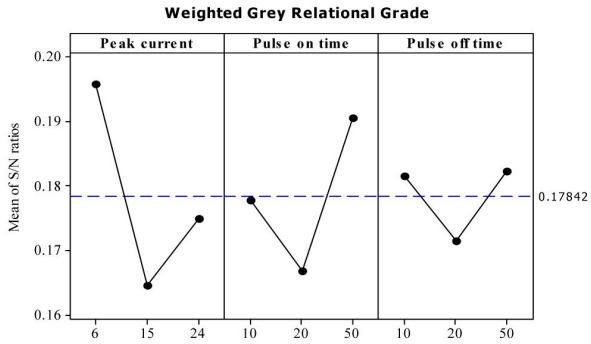

Fig. 3 Response plot of WGRG

4.1. Confirmation Experiments

The confirmation experiments are carried out at optimal levels A1B3C3. The results are compared with initial parameter levels A1B2C1 as given in Table 9. The additive model is used to evaluate the predicted WGRG (η_{pred}) and given as,

$$\eta_{pred} = \eta_m + \sum_{i}^{j} \left(\eta_{jm} - \eta_m\right) \qquad (10)$$

where, η_{jm} is average WGRG at optimal levels, j is the number of parameters that affect WGRG and η_m is the overall average of WGRGs. It can be observed from Table 9 that WGRG improved from 0.1833 to 0.2130 i.e. machining performance is improved by 16.20%. TWR is decreased from 3.61mg/min to 0.9433mg/min and MRR increased from 78.53mg/min to 106.76 mg/min. ROC increased from 0.159mm to 0.184mm. Sometimes, one of the response becomes poor while carrying out multi-response optimization and the same has been observed in the present study.

5. SEM, EDAX AND XRD ANALYSIS

SEM micrographs are taken at optimal levels of ROC and MRR and are shown in Fig. 4. Surface characteristics in Fig. 4(a) show small and tiny craters with few globules of debris, and less amount of appendage that result in better surface integrity. Fig. 4(b) shows huge uneven craters with lots of globules of debris, appendages and cracks on the entire machined surface, resulting in damage to surface integrity and responsible for higher surface roughness. In addition, EDAX analysis at A3B3C3 levels is shown in Fig. 5 and it is found that there is no transfer of copper particles from tool electrode and carbon percentage is more compared to parent material because pyrolytic carbon particles are formed at higher discharge energy levels. Also XRD patterns of unmachined surface and machined surface at optimum levels A3B3C3 respectively are shown in Fig. 6. It shows Ti_3AlC phase-basic matrix strengthener, Al-Ni-C carbide phase; Al-Ni-Ti and Fe-Ni-Ti solid solutions all belong to parent material. The patterns do not have any oxides of Ni, Al and

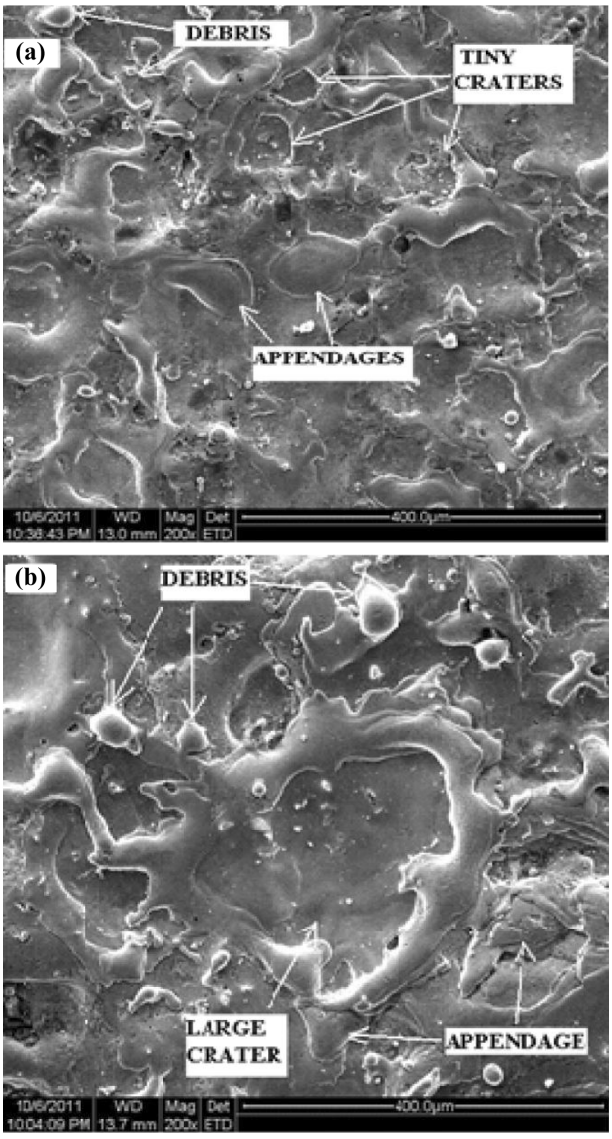

Fig.4 SEM micrographs at levels (a) A1B1C1 (b) A3B3C3

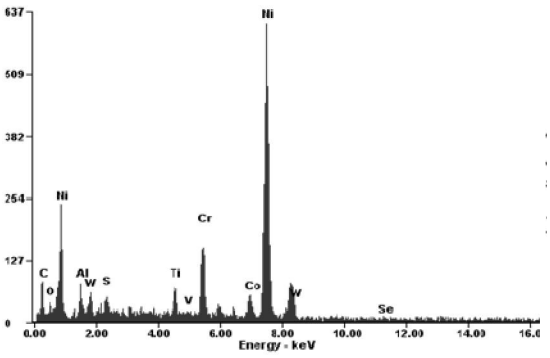

Fig. 5 EDAX pattern at levels A3B3C3

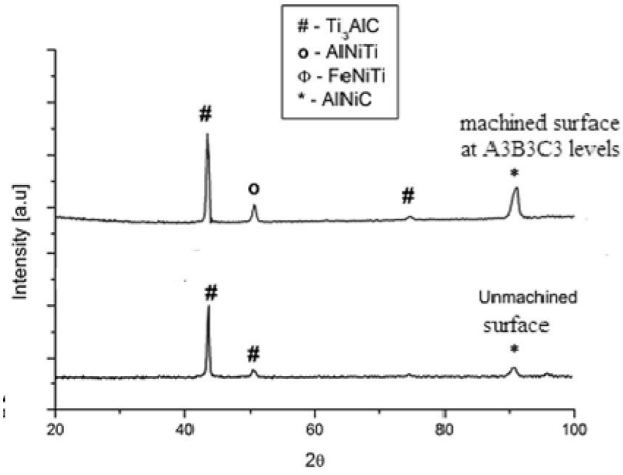

Fig. 6 XRD patterns

Cr etc. In short, there is rarely any difference between phases of unmachined surface and machined surface at A3B3C3 levels.

Further, the SEM views of surfaces machined at initial parameter levels A1B2C2 and optimal levels A1B3C3 obtained by TGRA are shown in Fig. 7(a) and Fig. 7(b) respectively. Fig. 7(a) reflects surface defects such as thick appendages around the craters, melted drops and globules of debris adhered to the machined surface. Also it shows number of pock marks and bigger craters. Fig. 7(b) indicates that the intensity of appendages, melted drops and globules of debris is relatively less due to optimal condition. Also, it shows less pockmark features and smaller craters. EDAX analysis at optimal levels A1B3C3 is shown in Fig.8 and it indicates that there is no carbon element unlike in Fig.5 and there is no transfer of copper electrode particles. The XRD pattern of machined surface taken at optimal levels is shown in Fig.9 and it reveals the phases like Ti_3AlC and $Ni_3(Al, Ti)$ which belong to parent material. This means that there is no change in phases of alloy of machined surface and unmachined surface.

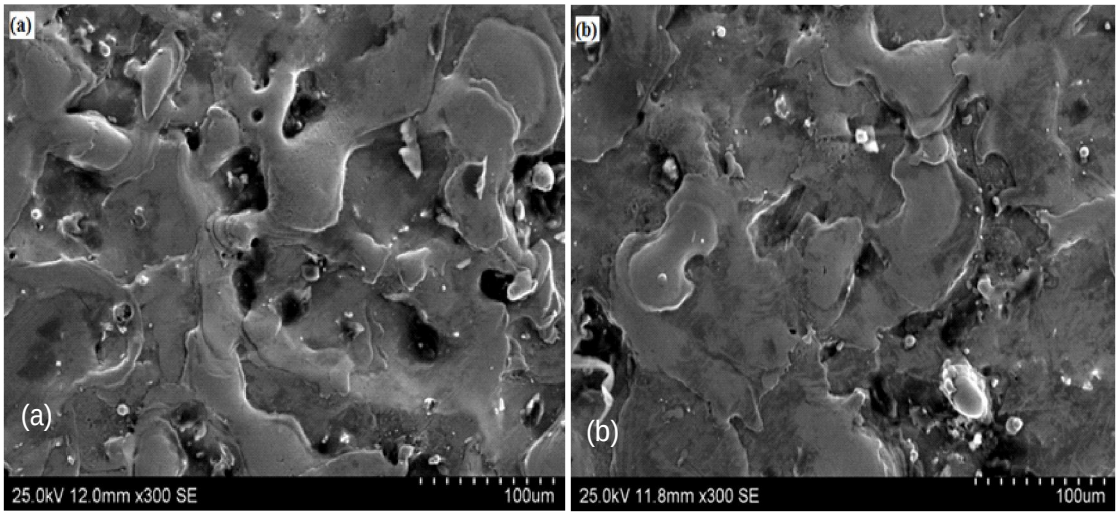

Fig. 7 SEM micrographs of machined surface at 300X, with (a) initial levels at A2B1C2 (b) optimal levels at A1B3C3

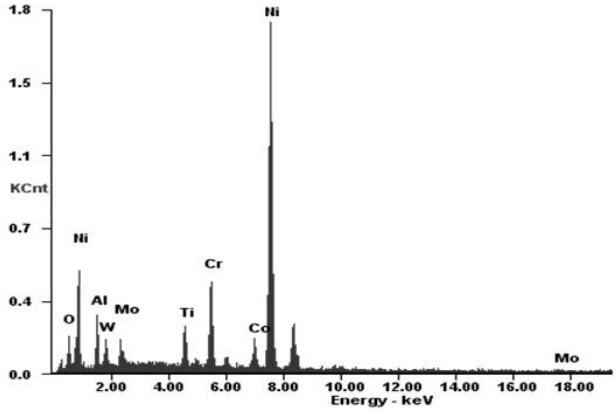

Fig. 8 EDAX analysis at optimal levels A1B3C3

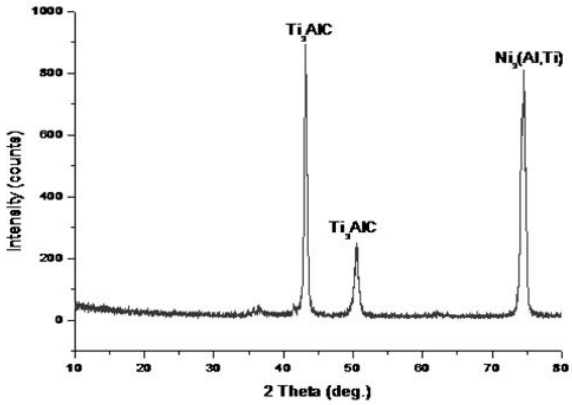

Fig.9 XRD pattern of machined surface at optimal levels- A1B3C3

6. CONCLUSIONS

The effect of peak current, pulse on time and pulse off time on ROC, TWR and MRR is studied. It is observed that peak current is more predominant parameter among the three. ROC increases with increase of peak current and pulse on time. TWR increases with increase of peak current and decreases with pulse on time. MRR increases with increase of all three parameters. Optimal levels of process parameters for multi-response optimization are A1B3C3 using TGRA. TWR and MRR increased by 73.86% and 35.94% respectively and ROC increases by 15.72%. Surface integrity of the alloy includes white layer, debris, appendages and voids. There is no transfer of copper electrode particles to the machined surface and no formation of oxides at optimal parameter levels in EDM environment.

REFERENCES

[1] Choudhary, I.A. and El-Baradie, M.A., Machinability of Nickel Base Super Alloy:

A General Review, Journal of Materials Processing Technology, Vol. 77, pp.278-284, 1998.

[2] Ho, K.H. and Newman, S.T., State of the Art Electrical Discharge Machining (EDM), International Journal of Machine Tools and Manufacture, Vol. 43, pp. 1287-1300, 2003.

[3] Pradhan, B.B., Masanta, M., Sarkar, B.,R. and Bhattacharya, B., Investigation of Electro-Discharge Micro-Machining of Titanium Super Alloy, International Journal of Advanced Manufacturing Technology, Vol.41, pp.1094-1106, 2009.

[4] George, P.M., Raghunath, B.K., Manocha, L.M. and Ashish M.W., EDM Machining of Carbon-Carbon Composite – A Taguchi Approach, Journal of Material Processing Technology, Vol.145, pp.66-71, 2004.

[5] Kumar, A., Sai Srinadh, K.V. and Nikalje, A.M., Optimization of EDM Machining Parameters of Maraging Steel (MDN300) Using Taguchi Method, Proceedings of the 24th AIMTDR Conference, Visakhapatnam, pp.265-270, 2010.

[6] Kao, Y.C., Tsao, S.S. and Hsu, Y., Optimization of the EDM Parameters on Machining Ti-6Al-4V with Multiple Quality Characteristics, International Journal of Advanced Manufacturing Technology, Vol.47, pp.395-402, 2010.

[7] Aliakbari, E. and Baseri, H., Optimization of Machining Parameters in Rotary EDM Process by Using the Taguchi Method, International Journal of Advanced Manufacturing Technology, doi: 10.1007/s00170-011-3862-9, 2012.

[8] Phadke, M.S., Quality Engineering Using Robust Design, Prentice Hall, New Jersy, 1989.

[9] Kibria, G., Sarkar, B.R., Pradhan B.B. and Bhattacharya, B., Comparative Study of Different Dielectrics for Micro-EDM Performance during Microhole Machining of Ti-6Al-4V, International Journal of Advanced Manufacturing Technology, Vol. 48, pp.557-570, 2010.

[10] Rajesha, S., Sharma, A.K. and Kumar, P., On Electro Discharge Machining of Inconel 718 with Hollow Tool, Journal of Materials Engineering and Performance, doi: 10.1007/s11665-011-9962-8, 2010.

[11] Banerjee, S., Mahapatro, D. and Dubey, S., Some Study on Electrical Discharge Machining of ({WC+TiC+TaC/NbC}-Co) Cemented Carbide, International Journal of Advanced Manufacturing Technology, Vol.43, pp.1177- 1188, 2009.